ACS APPLIED MATERIALS & INTERFACES

Applications of Polymer, Composite, and Coating Materials

A new method towards a robust covalently attached cross-linked nanofiltration membrane

Nikos Kyriakou, Renaud Merlet, Joshua D. Willott, Arian Nijmeijer, Louis Winnubst, and Marie-Alix Pizzoccaro-Zilamy

ACS Appl. Mater. Interfaces, **Just Accepted Manuscript** • DOI: 10.1021/acsami.0c13339 • Publication Date (Web): 25 Sep 2020

A new method towards a robust covalently attached cross-linked nanofiltration membrane

Nikos Kyriakou[†], *Renaud B. Merlet*[†], *Joshua D. Willott*[ł], *Arian Nijmeijer*[†], *Louis Winnubst* [†] *and Marie-Alix Pizzoccaro-Zilamy* [†,]*

[†]Inorganic Membranes, Membrane Science and Technology Cluster, University of Twente, P.O. Box 217,7500 AE Enschede, The Netherlands

[ł]Membrane Surface Science, Membrane Science and Technology Cluster, University of Twente, P.O. Box 217,7500 AE Enschede, The Netherlands

KEYWORDS click chemistry, nanofiltration, porous ceramic support, ultrathin membrane, molecular separation, liquid-vapor interfacial polymerization, thioether-based network.

ABSTRACT: As nanofiltration applications increase in diversity, there is a need for new fabrication methods to prepare chemically and thermally stable membranes with high retention performance. In this work, thio-bromo "click" chemistry was adapted for the fabrication of a robust covalently attached and ultrathin nanofiltration membrane. The selective layer was formed on a pre-functionalized porous ceramic surface via a novel, liquid-vapor interfacial polymerization method. Compared to the most common conventional interfacial polymerization

procedure, no harmful solvents and a minimal amount of reagents were used. The properties of the membrane selective-layer and its free-standing equivalent were characterized by complementary physico-chemical analysis. The stability of the thin selective layer was established in water, ethanol, non-polar solvents and up to 150°C. The potential as a nanofiltration membrane was confirmed through solvent permeability tests (water, ethanol, hexane, toluene), PEG-in-water molecular weight cut-off measurements (≈700 g mol^{-1}) and dye retention measurements.

Introduction

Separation, recovery and disposal of liquid mixtures in industry accounts for at least 40 – 70% of both capital and operating costs.[1,2] Membrane-based technologies have shown potential as alternative or complement of conventional separation and purification processes thanks to their easy operation, high separation efficiency, low energy consumption, and eco-friendliness.[3] This has been observed particularly for the purification of water or organic solvents under extreme process conditions (e.g. high pressure and/or temperature),[1] where nanofiltration (NF) membranes are ideal for the removal of small organic solutes with a molecular size between 0.5 and 2 nm (like antibiotics, catalysts etc.).

Interfacial polymerization (IP) is extensively used for the preparation of NF membranes. This method allows the formation of ultrathin dense polymeric networks on porous substrates by a controlled polymerization process at the interface of two immiscible phases (e.g. water-toluene).[4,5] Unfortunately, the fabrication of NF membranes with good separation performance by IP implies the use of solvents and monomers in a large excess[6] (e.g. at least 1 – 3 wt.%) due

to the low monomer to polymer conversions[7] and byproduct formation. As a result, large quantities of waste are produced, which is one of the major drawbacks of the IP method.[8]

Also, despite the excellent performance reported for the NF membranes prepared by the IP method, the resulting polymeric layers present a low mechanical and chemical stability under severe conditions (i.e., extreme pH values, bleach, and other reactive chemicals).[9,10] This correlates to the monomers used which are usually composed of halogenated acids, such as trimesoyl chloride (TMC), and diamine benzene-derivatives (DAB). A combination of these types of monomers facilitates the formation of crosslinked polymeric networks at short reaction times, which leads to enhanced chemical stability in polar and apolar solvents. However, the amide bonds formed during the reaction between these two types of monomers (TMC and DABs) are very sensitive to hydrolysis and cannot thus withstand strong acids, bases, or hypochlorite-based cleaning treatments.[11,12] Additionally, swelling and detachment of the membrane from the porous substrates can occur during the cleaning treatment as the conventional IP process does not involve a covalent attachment between membrane and the substrate surface. Therefore, there is a need to adjust the IP reaction process to mitigate waste production and to increase the chemical and mechanical stability of the NF membranes produced.

To overcome the challenges of conventional IP methods, “click” chemistry can be used instead of amidization reactions. “Click” chemistry is a tool used for the fabrication of highly cross-linked and chemically stable polymers. This method is characterized by a high reaction yield and low waste production.[13] Besides, “click” reactions can promote the formation of chemical linkages that are chemically inert even under extreme conditions. Among the existing possibilities, the thio-bromo “click” reaction, which occurs at room temperature under basic

conditions (pH < 9), results in stable thioether bonds which can be used as an alternative to conventional amidization reactions used in conventional IP methods.

In 2005, Timmerman *et al.*[14] established the first thio-bromo "click" reaction synthesis to prepare cyclic peptides in high yields and more rapidly than conventional synthesis methods. The resulting products were made via the reaction of cysteine-based peptides as thiol substituted with benzylic bromides under mild basic conditions (pH ~8).[15] The method was expanded to the preparation of polymers by Monnereau *et al.* in 2015.[16] Hyper-crosslinked thioether-based porous polymers were formed under similar conditions. These networks were shown to be insoluble in common organic solvents and were thermally stable up to 500 °C. "Click" reactions show great potential for use in membrane technology due to the simplicity, the high yields of the reaction conditions, and the resulting chemical stability of the polymers formed. Most studies using "click" chemistry focused on minor precursor modifications either before[18–20] or after[21,22] the layer formation. However, thus far no study has used the powerful and high yielding "click" reactions to form distinct membrane selective layers. Therefore, by adapting the IP method with the "click" reactions, ultrathin and selective membrane layers can be formed. A proof of concept was shown by Rapakousiou *et al.* in 2017,[17] where the liquid/liquid IP method in combination with the "click" reaction of copper-catalysed azide-alkyne cycloaddition (CuAAC) was used to form an ultrathin polymer with thickness of 5 nm. In this work, we propose a novel method towards the formation of an ultrathin cross-linked NF membrane composed of stable thioether bonds. Starting from the top surface of a pre-functionalized porous ceramic support, two successive thio-bromo "click" reactions are conducted to form the NF separation layer. Here, the "click" reaction is also used to covalently attach the polymeric layer on top of a porous ceramic support. Ceramic supports, which exhibit high thermal and chemical stability, do not suffer from

plasticization issues, swelling, or thermal degradation; phenomena observed with common porous polymeric supports. In addition, ceramic supports can be easily functionalized with a wide range of small organic molecules[21] including thiol-terminated ones.[22] Even though IP layers have been successfully formed on ceramic supports in the past,[23] only conventional IP (polyamides predominantly) procedures were used and to-date no covalent attachment between selective layer and the ceramic support has been reported. In this work the second "click" reaction is done via a vapor phase reaction without the use of a catalyst. For the first time we report a selective layer made completely *via* "click" chemistry. A special effort is devoted to understanding the impact of each reaction step on the final layer as well as the thermal and chemical stability of the network. The system reported here can serve as a proof-of-concept for developing thioether-based layers for a wide range of applications such as in membrane science, coatings, optoelectronics and many more.

Materials & methods

Materials

Solvents used were ethanol (technical grade > 95%), anisole (>99%, Merck, NL), and water (MilliQ). Chemicals used were glycerol (anhydrous, Merck, NL), 1,3,5-tris(bromomethyl)benzene (3Br) (> 97%, Fluorochem, UK), (3-mercaptopropyl)trimethoxysilane (MPTMS) (> 95%, Merck, NL), 1,3-benzenedithiol (2SH) (> 99%, Merck, NL), triethanolamine (TEOA) (> 99.5%, Merck, NL), Brillant Yellow (70%, Sigma Aldrich, NL), Rhodamine B (> 99%, Meck, NL), Sudan Black B (> 99%, Sigma-Aldrich, NL), polyethylene glycol (Merck, NL). The chemical structures and abbreviations can be found in Figure S1 of the Supporting

Information. The α-alumina (α-Al_2O_3) substrates (disc: 21 or 39 mm of diameter, 2 mm of thickness, 80 nm pore diameter) were purchased from Pervatech B.V., the Netherlands. These ceramic substrates are comprised primarily of macroporous α-alumina (> 99 %), which ensures mechanical stability under pressure. The polished side of these supports was dip-coated with a boehmite sol and subsequently calcined at 650 °C for 3 hours. The procedure was performed twice to eliminate any defects on the surface of the γ-alumina support and led to the formation of a thin γ-alumina layer of 3 μm in total thickness (Figure S2.B of the Supporting Information). Further details for the fabrication of the γ-alumina coated support can be found elsewhere.[24-26]

Thioether-based cross-linked NF membrane preparation

Prior to use the mesoporous γ-alumina supports, these were soaked in a water/ethanol mixture (v/v = 2:1) for 8 h before drying under vacuum at 50°C. The synthesis of the thioether-based cross-linked membrane is divided in three steps as described in Scheme 1.

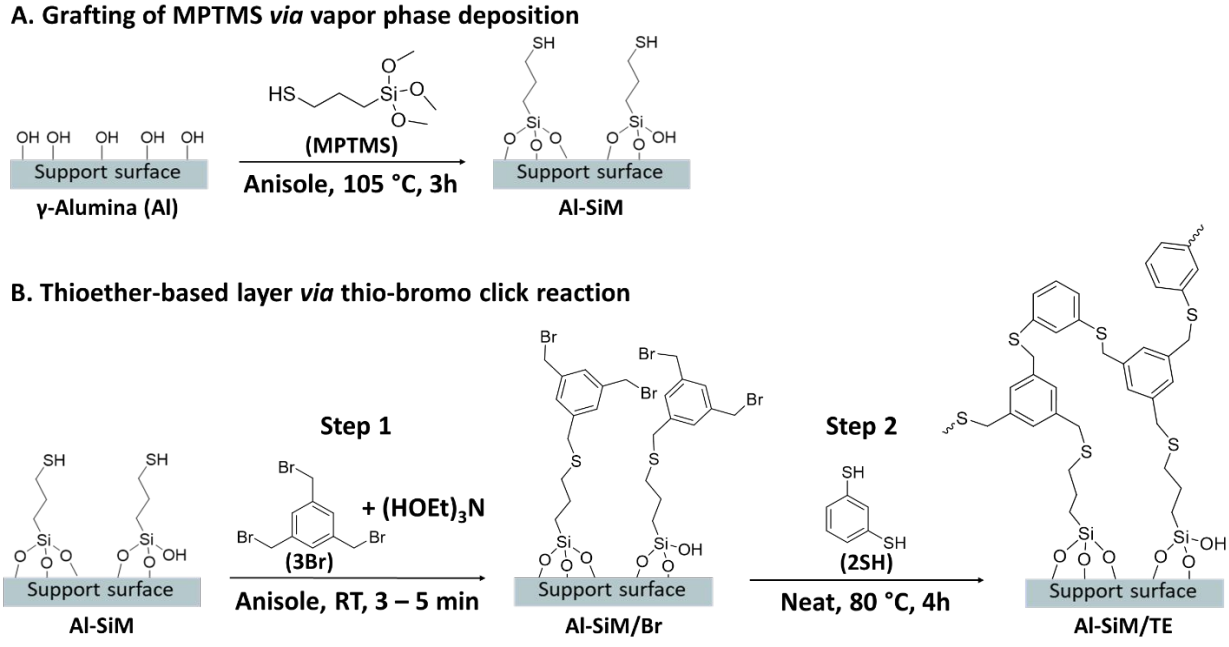

Scheme 1. Schematic representation of the grafting of MPTMS via vapor phase deposition (A) and the stepwise thioether-based membrane formation (B).

Porous support pre-functionalization: The grafting of (3-mercaptopropyl)trimethoxysilane (MPTMS) was conducted using the vapor phase grafting method. Prior the synthesis, γ-alumina support was filled with glycerol by rubbing a drop (≈1 mL) onto the substrate surface and after 10 min stand time, dabbed with a tissue. Vapor phase grafting was conducted by placing a glycerol-filled γ-alumina support (top-surface facing down) 2 – 3 cm above 50 mL of a 25 mM anisole solution of MPTMS at 105°C for 3h (Figure S4). After cooling to room temperature, the pre-functionalized porous support was washed with 20 mL anisole for 1h under sonication to remove the physisorbed species, and dried overnight at 50°C under vacuum. Samples obtained at this stage were denoted Al-SiM.

Liquid phase "click" reaction: Following the MPTMS grafting step, the pre-functionalized porous support was soaked for 3 – 5 min in a solution containing 0.22 mmol of 1,3,5-tris(bromomethyl)benzene (3Br) and 0.16 mmol of triethanolamine (TEOA) in 10 mL of anisole (Figure S4). After removing from the solution, compressed air was gently blown across the surface of the support to remove any solvent visible to the eye. Samples obtained at this stage were denoted Al-SiM/Br.

Vapor phase "click" reaction: The thioether-based cross-linked membrane was then prepared by placing the Al-SiM/Br samples (top-surface facing down) 1 – 2 cm above 25 µL (0.17 mmol) of 1,3-benzenedithiol (2SH) pure precursor at 80°C for 4h under stirring (Figure S4). After cooling to room temperature, the resulting membrane was washed twice in 20 mL of ethanol for

30 min under sonication and dried at 50°C under vacuum. Samples obtained at this stage were denoted Al-SiM/TE.

Characterization

Fourier Transform Infrared spectroscopy (FTIR) measurements were done using a Perkin Elmer UATR Spectrum Two. Wavenumbers between 4000 and 550 cm^{-1} were scanned in reflectance mode at a resolution of 4 cm^{-1} for a minimum of 16 scans.

Field-emission scanning electron microscopy (FE-SEM) images were obtained with a Zeiss MERLIN high-resolution scanning electron microscope using an accelerating voltage of 1.4 kV. FE-SEM samples were sputtered with 2 nm of chromium to avoid sample charging.

Thermogravimetric analysis (TGA) coupled with differential scanning calorimetry (DSC) and mass spectroscopy (MS) was conducted using an STA 449 F3 Jupiter (Netzsch), equipped with a dual TG/DSC sample/reference holder. Measurements were performed under 55 mL min^{-1} N_2 and 15 mL min^{-1} O_2 flow with a heating rate of 10 °C min^{-1} from 40 to 800 °C. Calibrations were made using melting standards. Measurements were run sample-temperature controlled. The sample masses were determined using an internal balance 30 min after inserting the sample. The gases evolved during TGA analysis were transferred to a mass spectrometer (QMS 403 D Aëolos, Netzsch). TGA and MS start times were synchronized, but no correction was applied for the time offset caused by the transfer line time (estimated < 30 s, systematic offset). A bar graph scan for m/z = 1–110 amu was recorded for all samples to determine the evolving m/z numbers. TGA/DSC crucible correction can be found in Supporting Information, Figure S12.

Pore size of the mesoporous alumina membranes was determined by permporometry using cyclohexane as condensable vapor. The experimental procedure is described in detail elsewhere.[27]

X-ray fluorescence spectroscopy (XRF) measurements were conducted on a Bruker SS Tiger using membrane samples prepared via the stepwise membrane method descripted above. Complete elemental analysis is provided in the Supporting Information.

Spectroscopic ellipsometry was performed using a J.A. Woollam M-2000 ellipsometer on silicon wafer (one side polished, CZ test grade, Silchem) samples coated in a fashion identical to the prepared Al-SiM, Al-SiM/Br and Al-SiM/TE membrane samples without the glycerol pre-treatment step. First, a piece of silicon wafer (30x30 mm) with a native oxide layer was cleaned in an oxygen plasma chamber for 10 min at 100 watts. Any residual organics were washed off with ethanol and then, the wafer was dried under vacuum at 50 °C overnight. The preparation of the coatings followed the stepwise protocol developed for the preparation of the thioether-based membrane except that no pore-filling agent was used. After each reaction step, a part of the substrate was preserved for the analysis (Figure S13). Each sample was rinsed with ethanol multiple times and dried under vacuum overnight at 50 °C and stored under N_2 at room temperature. The detailed parameters to assess the layer thickness can be found in the Supporting Information.

Membrane screening and performance tests

Permeability and retention data were collected with a custom-made, dead-end filtration setup, consisting of a nitrogen tank pressurizing a feed vessel with a valve to regulate pressure.

Permeability is expressed as the flux of water or a solvent across a membrane per unit of driving force, here as liters per square meter of exposed membrane area (2.4 or 9.1 cm^2) per hour per bar of pressure applied across the membrane (L m^{-2} h^{-1} bar^{-1}). Permeability data were collected by weighing the flow of permeate at timed intervals and at three applied transmembrane pressures between 8 and 15 bar, and by taking the slope of a linear fit of the collected data. All slopes were found to be linear unless otherwise noted. A permeability of 0.0 indicates no detected solvent flux during 17 h of operation at a transmembrane pressure of 15 bar.

Retentions (R) of Brilliant Yellow (BY, Mw = 624.55 g mol^{-1}, 50 ppm), Rhodamine B (RB, Mw = 479.02 g mol^{-1}, 50 ppm), Sudan Black B (SBB, Mw = 457 g mol^{-1}, 50 ppm) or PEG oligomers (Mw = 300, 600, 1000, 1500 g mol^{-1}) were calculated by the equation

$$R = 1 - c_p/c_f \quad (1)$$

where c_p and c_f are the permeate and feed solute concentrations, respectively. Retention samples were obtained at recoveries between 15-25%. Solute concentrations of BY, RB and SBB were calculated from Perkin-Elmer λ12 UV-Vis spectrophotometer results at the characteristic wavelength of 401.5 (BY), 554 (RB) and 604 (SBB) nm. PEG concentrations were determined by gel permeation chromatography (GPC). The GPC setup consisted of two SUPREMA 100 Å columns from PSS Polymer Standards Service GmbH (Germany), an HPLC pump from Waters (Millipore B.V., The Netherlands) and a Shodex RI-Detector from Showa Denko GmbH (Germany). The columns were calibrated using the same PEG standards.

Results and Discussion

Porous support pre-functionalization with MPTMS

The porous γ-alumina top-surface was pre-functionalized with 3-(mercaptopropyl)trimethoxysilane (MPTMS), a precursor for the thioether-based network, using a vapor phase deposition grafting method (Scheme 1A). Here, the alkoxysilane linking groups of the precursor react with the hydroxyl-rich surface of the γ-alumina support via a condensation reaction, yielding a homogeneous monolayer coverage without poly(homo)condensation reactions.[21]

FTIR analysis was used to demonstrate the grafting of the MPTMS precursor on the top-surface of the porous γ-alumina support. The FTIR spectrum of the pristine (Al) and pre-functionalized γ-support (Al-SiM) in the range 3800 – 2300 cm^{-1} and 1800 – 960 cm^{-1} are presented in Figure 1A and 1B. The bands appearing on the Al-SiM spectrum between 2840 and 2950 cm^{-1} correspond to the symmetric and antisymmetric C–H stretching vibrations of the precursor's aliphatic group. The grafting is suggested by the disappearance of a sharp vibration band at 2840 cm^{-1} which corresponds to the Si-O**CH_3** group of the MPTMS precursor (Figure S11, Supporting Information, section 5). This is also confirmed by the presence of a broad vibration band centered at 1050 cm^{-1} on the Al-SiM spectrum, which can be ascribed to the newly formed Si-O-Al bond and is not visible in the spectrum of the pristine support (Al).[28] Compared to the FTIR spectrum of the precursor, the weak stretching vibration band of the thiol group (**S-H**) located at 2565 cm^{-1} is not visible for the Al-SiM sample. This can be due to the low concentration of grafted molecules on the pre-functionalized surface and the weak absorbance of the S-H group in this IR region.[29] `

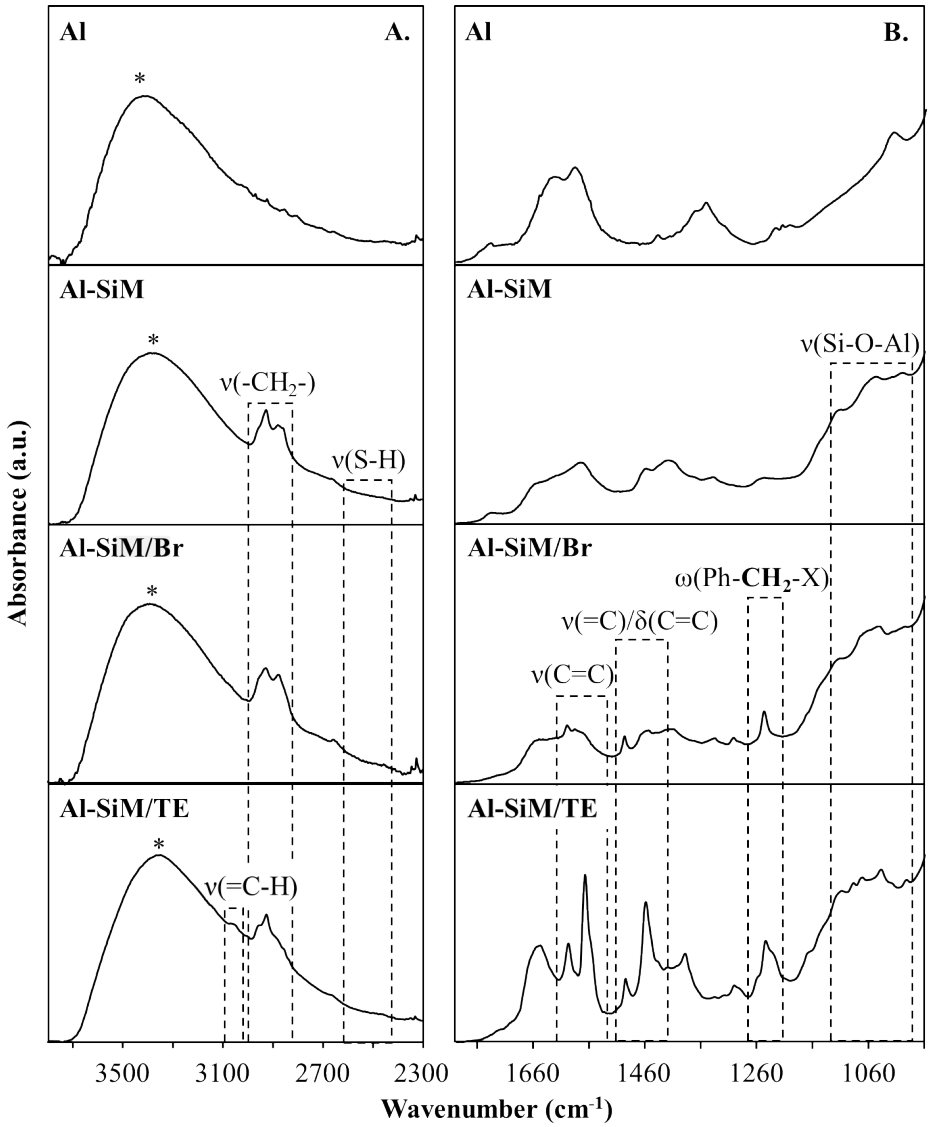

Figure 1. FTIR spectra of the Al, Al-SiM, Al-SiM/Br and Al-SiM/TE samples between 3800 – 2300 cm^{-1} (A) and 1800 – 960 cm^{-1} (B). The symbol (*) denotes the vibration band attributed to physiosorbed water.[23]

XRF was used to further confirm the presence and conservation of the side chain of the MPTMS precursor after grafting. The results are presented in Table S1 (Supporting Information, section 6). The analysis revealed the presence of silicon and sulfur, respectively 0.3% and 0.3%;

thus, confirming along with the FTIR results that the support has been successfully functionalized.

Cyclohexane permporometry was used to investigate the possible blocking of the support pores due to poly(homo)condensation reactions of the MPTMS precursor. Indeed, the presence of precursors into the pores can affect the formation and properties of the resulting NF thioether-based membrane. The oxygen flux through the Al-SiM and the unmodified γ-alumina support as a function of the relative cyclohexane pressure during the desorption step of the permporometry analysis is shown in Figure S13A (Supporting Information, section 7). At the beginning of the desorption step, all the pores are blocked with condensed cyclohexane and there is no oxygen flux. In the interval $0.5 > P/P_0 > 0.3$, the oxygen permeance increases with the increase in number of open pores. By considering that the capillary condensation process takes place in this interval, Kelvin diameters of ~5.5 and ~5 nm (Supporting Info, section 7) were calculated for the unmodified γ-alumina support and the Al-SiM sample (5.5 ± 0.03 and 4.8 ± 0.07, accordingly). The results are very similar, and we can thus conclude in the successful grafting of MPTMS on support's top-surface without poly(homo)condensation reactions into the pores.

Formation of the thioether-based hyper cross-linked membrane

Prior to the membrane fabrication, thioether-based free-standing films were prepared as a proof-of-concept via the liquid-liquid IP (LIP) method. The LIP method, in contrast to a single solvent system, allows for formation of a well-defined organic network.[30] Preparation of LIP free-standing films was proven to be crucial in determining potential side reactions by ^{1}H liquid NMR and the physico-chemical properties of the membrane layer such as thermal and chemical

stability. The preparation procedure and the physico-chemical characterizations of the film is reported in the Supporting Information (section 4).

Thioether-based cross-linked membranes were prepared on the pre-functionalized support (Al-SiM) in two steps, as shown in Scheme 1B. The first step consisted in the deposition of a basic solution of the 1,3,5-tris(bromomethyl)benzene (3Br) monomer onto the pre-functionalized porous ceramic support. Under these solution phase conditions, the thiol surface groups of the grafted precursors can react with the 3Br monomer via the thio-bromo "click" reaction, forming a thioether bond (Al-SiM/Br). The base catalyst (TEOA, $pK_a \approx 11$)[31] was added to the 3Br monomer solution to minimize the formation of disulfide bonds, which were detected by ^{1}H liquid NMR during the preparation of the film (Figure S9 and S10, Supporting Information, section 4). Disulfide bonds are in general weaker than thioether bonds since they can be cleaved under mild conditions[32,33] and thus their presence in the final membrane layer is viewed as defects. Subsequently, the support surface was exposed to 1,3-benzenedithiol (2SH) monomer vapors, leading to the formation of a thioether-based cross-linked membrane (Al-SiM/TE, Scheme 1B, step 2). This second step, was done without the use of base catalyst since the nucleophile in the vapor phase has enough energy to overcome the kinetic barrier of the "click" reaction.[34,35] Therefore, the 2SH monomer in the vapor phase is expected to react with the 3Br monomer in contact with the liquid phase. Thus, we expect that the "click" polymerization reaction occurs at the liquid-vapor interface and thus an interfacial polymerization should take place on top of the ceramic support. The reaction parameters for the preparation of Al-SiM/TE sample (Scheme 1B) were selected by screening through different reaction conditions (reaction times, and monomer concentrations). A combination of Sudan Black B (Mw = 457 g mol^{-1}) retention tests and solvent permeability measurements were conducted to identify the samples

showing the presence of a distinct selective and permeable layer on top of the support. The results of this preliminary study are summarized in the Supporting Information (section 8).

To confirm the formation of the thioether-based cross-linked network, FTIR analysis was conducted after each reaction step, on the respective samples Al-SiM/Br and Al-SiM/TE. The FTIR spectra in the range 3800 – 2300 cm^{-1} and 1800 – 960 cm^{-1} are presented in Figure 1A and B respectively. For these samples, the presence of aromatic rings is confirmed by the quadrant stretching vibration band observed at 1602 cm^{-1} (ν(C=C)). Moreover, this assumption is also verified by the multiple bands appearing at 1484, 1450, 1440 and 1412 cm^{-1} which are associated with the stretching and bending vibrations of the aromatic rings (ν(C=C) and δ(=CH)).[29,36] The good signal resolution of these vibration bands in the case of the Al-SiM/TE sample suggests the increase in concentration of aromatic rings, as compared to the Al-SiM/Br sample, which is attributed to the vapor phase "click" reaction (Scheme 1B, step 2). The absorption band at 1249 cm^{-1}, appearing in both samples, is attributed to the wagging vibration of the methyl group at the benzylic position, Ph-$\mathbf{CH_2}$-X, where X is either a sulfur or a bromine atom.[37] To determine if this vibration band resulted from the formation of thioether bonds or unreacted 3Br monomers, the spectra were compared to the spectrum of the pure 3Br monomer (Figure S14, Supporting Information, section). Even though, in the spectrum of the 3Br monomer, the vibration of the methyl group (Ph-$\mathbf{CH_2}$-Br) appears at 1209 cm^{-1}, the presence of the bromine in the Al-SiM/Br or /TE cannot be excluded and further in-depth analysis is required. Moreover, disappearance of the C-Br absorption band at 704 cm^{-1} would indicate full conversion of the benzylic bromides to thioethers in the membrane layer. However, no specific signals can be observed below 900 cm^{-1} in the case of the Al-SiM/TE membrane due to the high intensity of the signal attributed to the alumina support (Figure S14, Supporting Information, section 9). Here, the free-standing film

can be used since it is spectroscopically identical to the Al-SiM/TE. According to the FTIR of the film, an absorption band at 710 cm^{-1} is present which can be attributed to both unreacted methyl bromides (C-Br)[29] or the desirable thioether bonds (C-S-C).[38,39] Thus, from the FTIR results thioether-bond formation is indicated, however the presence of bromide in the sample cannot be excluded and further investigation is necessary.

XRF analysis was conducted to determine the amount of sulfur and the presence of any residual bromine in the final thioether-based membrane. The results are given in Table S1 (Supporting Information, section 6). The weight concentration of sulfur is increasing by 1.3% between the Al-SiM and Al-SiM/TE samples which confirms the increase concentration of thioether bonds on the surface (Al-SiM: 0.3 wt%; Al-SiM/TE: 2.0 wt%). Less than 0.1 wt% of bromine was detected in the Al-SiM/TE sample which suggests the predominance of the thioether-based bond formation.

To study the pore size of the membrane and to confirm the formation of a defect-free layer as suggested by the preliminary SBB retention tests, cyclohexane permporometry experiments were conducted. The oxygen flux through the Al-SiM/Br and Al-SiM/TE samples as a function of the relative cyclohexane pressure during the desorption step is shown in Figure S13A and B of the Supporting Information (section 7). A pore diameter of ~4 nm is determined for the Al-SiM/Br sample which indicates a pore shrinkage of ~1 nm compared to the unmodified γ-alumina support. This decrease in pore diameter can be attributed to the presence of the 3Br monomers which have reacted in step 1 with the thiol surface groups, present at the pores entrance (Scheme 1B). Concerning the Al-SiM/TE sample, an oxygen permeance of 1×10^{-8} $mol\ s^{-1}\ m^{-2}\ Pa^{-1}$ was

obtained (Figure S13A). This value corresponds to the detection limit of the setup. The absence of a clear transition point in the cyclohexane permporometry curve suggests firstly the complete coverage of the γ-alumina porous support with the thioether-based network, and secondly that the Al-SiM/TE sample is mainly composed of micropores (pore diameter < 2 nm).

According to literature,[40-42] the pore size of the layer can also be estimated using retention tests of a series of PEG molecules with different molecular weights (Mw). It is known that PEG molecules can form spheres in solution of certain radius, which can be estimated via the Stokes-Einstein equation (2):

$$\text{Molecular radius (Å)} = 0.1673 \times (M_w \text{ (g/mol)})^{0.557} \quad (2)$$

where M_W is the molecular weight of the PEG which is 90% retained by the membrane.

Figure S15 in the Supporting Information (section 10) shows the PEG retention obtained for the Al-SiM/TE sample. A molecular weight cut-off (MWCO) of ≈700 g mol^{-1} was obtained which is much lower the MWCO of unmodified γ-alumina support (2500 g mol^{-1}),[43] and well in the nanofiltration range.[1] Using the MWCO and the equation (2), a hydrodynamic diameter of 1.3 nm was calculated. This value is in accordance with the pore diameter suggested by the cyclohexane permporometry measurements (pore diameter below 2 nm) and in the pore range needed for NF applications.

FE-SEM analysis was used to investigate the morphology, location, and homogeneity of the Al-SiM/TE membrane. Figure 2A shows a cross-section image of the membrane with part of the α-alumina support and the γ-alumina layer consistent with reported characteristics.[24,25] No

organic layer was observed on the top surface until higher magnification was used, as shown in Figure 2B, where a thin organic layer is indicated. The organic layer seems to be in direct contact with the γ-alumina support. However, as shown in Figure 2B, the top layer also appears in a different location in the form of thin flakes detached from the supports. The detachment can be artefacts induced either by the primary electron beam or the high vacuum of the SEM equipment. Based on these observations, the layer thickness should not be more than 50 nm.

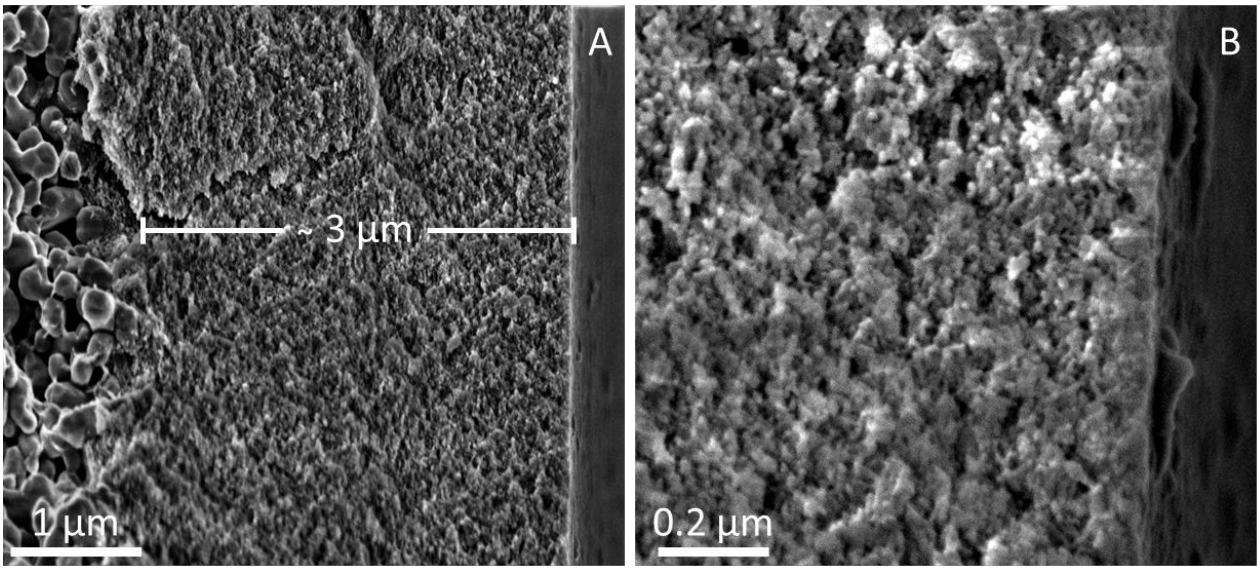

Figure 2. FE-SEM cross section images of the thin thioether-based membrane layer covalently attached to a mesoporous γ-alumina support with a magnification of 63k (A) and 260k (B).

For insight into the thickness of the thioether-based layer, spectroscopic ellipsometry measurements were performed. Ellipsometry has been used to measure the thickness of polymeric film prepared by conventional LIP.[44] However, due to the roughness and porosity of the γ-alumina support it is impossible to apply this analysis to the Al-SiM/TE membrane. Thus, the membrane synthesis was transposed onto silicon wafer substrates to study layer formation

after each reaction step. Grafting of MPTMS on the silicon wafer yields a thin layer of 1.0 ± 0.1 nm. This thickness value is in accordance with MPTMS layers prepared by Gothe et al.[45] After the first "click" reaction with the 3Br monomer, an increase in thickness of ~0.3 nm was measured. Finally, after the second "click" reaction with the 2SH monomer by VIP an ultrathin thioether-based layer is formed with a thickness of 7.8 ± 0.4 nm. We expect that when prepared on the porous membrane support, the thickness of the thioether-based layer would be higher than the one shown by ellipsometry due to the inherent porosity of the γ-alumina support. Even though, the pores of the support are filled with glycerol, monomers are expected to be able to infiltrate the porous ceramic during the VIP step and to form a thicker layer than the one observed with ellipsometry. Nevertheless, the thickness of the membrane separation layer is expected to be very thin and thus would not be observed by FE-SEM.

Stability of the thioether-based cross-linked membrane

The stability of the thioether-based network was assessed first through exposure to different solvents. Permeability tests were conducted with solvents of different polarity (water, ethanol, toluene and hexane) under the same conditions. A thermal treatment was included in the test to study any potential degradation of the structure caused by the temperature or the solvent tested. As shown in Figure 3, the water permeability of the Al-SiM/TE membrane is approximately 0.60 ± 0.05 L m^{-2} h^{-1} bar^{-1} and similar to ethanol permeability (0.50 ± 0.02 L m^{-2} h^{-1} bar^{-1}). Compared to the water permeability of the γ-alumina coated support (6 L m^{-2} h^{-1} bar^{-1}) and the bare α-alumina (7 – 8 L m^{-2} h^{-1} bar^{-1}) support,[40] the thioether based membrane exhibits approximately one order of magnitude lower permeability, which suggests the presence of a layer on top of the support. The Al-SiM/TE membrane was found impermeable to apolar solvents, such as toluene

and hexane. This suggests that either the organic layer has collapsed and a dense network has formed in contact with the apolar medium or the organic layer has a rigid hydrophilic structure, impermeable to apolar solvents. To ascertain which is the case, the membrane was dried and re-tested with water. As shown in Figure 3 the water permeability showed a slight change (0.53 L m^{-2} h^{-1} bar^{-1}), which is attributed to incomplete drying of the apolar solvents between the tests. However, the results suggest that thioether-based layer did not collapse in presence of apolar solvent. Thus, formation of a rigid hydrophilic network via the VIP method is indicated.

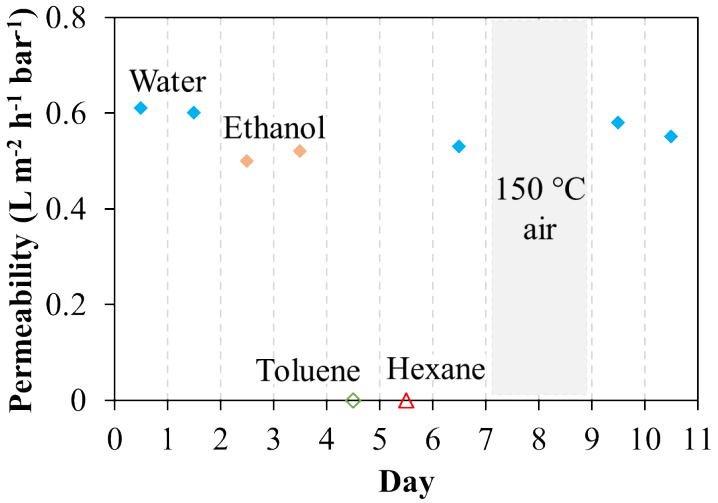

Figure 3. The permeability of various solvents through the same membrane over consecutive tests. The same membrane was exposed to heat for 2 days and then the water permeability was tested for 2 consecutive days. Between each permeability test the sample was dried overnight at 50 °C under vacuum.

Following the solvent permeability tests, the thermal stability of Al-SiM/TE membrane was further investigated. The sample was thermally treated at 150 °C during 48h and a water permeability of 0.57 L m^{-2} h^{-1} bar^{-1} was measured. This value is within error from the value obtained before the thermal treatment (0.53 L m^{-2} h^{-1} bar^{-1}).

To further confirm the integrity of the network, a free-standing film was analyzed by TGA-MS and FTIR spectroscopy. The TGA results indicate that the thioether-based layer is thermally stable below 300 °C, where no weight loss was observed (Figure S17, Supporting Information, section 13). Above 310 °C, thermal degradation occurs with a significant weight loss above 460 °C. FTIR analysis confirmed this observation (Figure S18, Supporting Information, section 14). Compared to the FTIR spectrum of the free-standing film, the thermally treated sample shows small differences in vibration bands. New weak bands at 2500, 1500 and 1150 cm^{-1} could be denoted, possibly due to a slight oxidation of the film. Overall, these results confirm that the thioether-based membrane prepared via the novel VIP method bear a highly dense and hydrophilic network thermally stable until at least 150 °C.

Membrane performance

A series of retention tests were conducted on the Al-SiM/TE membrane using aqueous solution of Brilliant Yellow (BY, 625 g mol^{-1}), Rhodamine B (RB, 479 g mol^{-1}) and an ethanolic solution of Sudan Black B (SBB, 457 g mol^{-1}). The results are given in Table 1. Both aqueous solutions result in high retentions values, 99 ± 0.4% for BY and 93 ± 7% for RB. However, SBB retention in ethanol averaged to 50 ± 2% which can be attributed to the neutral character of the SBB dye as compared to the charged BY or RB. This along with being impermeable to apolar solvents indicates that the Al-SiM/TE membrane bears a dense charged surface. Thus, we expect that the Al-SiM/TE membranes can find use in removal of dyes from water. Table S4 compares the retention performance vs. water permeability of the thioether-based nanofiltration membrane prepared in this work, with data from the open literature. For the sake of relevant comparison, only organically grafted- γ-alumina membranes were considered in this table. Indeed, the porous

ceramic support structure (pore diameter, porosity, architecture) play a strong role on the resistance to the solvent transport as reported in our previous work.[42] Compared to the literature, the thioether-based nanofiltration membrane present promising retention performance (PEG MWCO ~ 700 instead of 2800 Da) with an acceptable water permeability (~0.6 L m^{-2} h^{-1} bar^{-1}). To enhance the membrane permeability, our future research will focus on the adaptation of the membrane structure (intrinsic microporosity), and support (to decrease the resistance to the water flux).

Table 1. Solute rejection tests performed on the Al-SiM/TE membrane. The tests were performed under constant pressure (11 bar), using nitrogen gas, and stirring 700 – 800 rpm. Each test was reproduced three times of which the presented retention is the average and the error refers to the standard deviation from the average value of 3 samples.

Solute	Solvent	Charge	M_W (g mol^{-1})	Retention (%)
Brilliant Yellow	Water	Negative	625	100 ± 0.4
Rhodamine B	Water	Positive	479	93 ± 7
Sudan Black B	Ethanol	Neutral	457	50 ± 2

Conclusions

A "click" reaction approach within a novel liquid-vapor IP method was used to prepare ultrathin selective thioether-based cross-linked NF membranes. Here, we report for the first time the combination of "click" chemistry with interfacial polymerization in membrane preparation. In addition to that, we show the formation via means of "click" chemistry on a porous ceramic support and formation of a hybrid system, which in the best of our knowledge has never been

reported in literature before. Typically, LIP methodologies used in membrane technology rely on a biphasic liquid system, however our novel liquid-vapor system relies on a single environmentally friendly solvent and minimal reactant usage. The monomer amounts used in this work are very small (from 0.05 to 0.2 wt.%) when compared to concentrations of a typical IP procedure (from 1 to 3 wt.%).[6] We demonstrated, via spectroscopic and solvent permeation tests, that the thioether layer exhibits high thermal (150°C for two days) and chemical stability (ethanol, hexane, toluene).

Preliminary nanofiltration tests show permeabilities of 0.6 and 0.5 L m^{-2} h^{-1} bar^{-1} in water and ethanol, respectively with a PEG MWCO of 700 g mol^{-1} as well as good retention of charged dyes in water. The membrane was found to be impermeable yet stable to two apolar solvents, toluene and hexane. Based on this proof-of-concept, the development of thioether-based cross-linked networks can be expanded to a variety of NF and separation applications.[16] The liquid-vapor interfacial polymerization method presented is a highly effective and facile method which shows significant advantages over the liquid-liquid IP method.

ASSOCIATED CONTENT

Supporting Information. The Supporting Information is available free of charge on the ACS Publications website at DOI:.

The following files are available free of charge.

Chemical structures and abbreviations of the compounds used in this study, Mesoporous γ-alumina support, Schematic illustration for the thioether-based cross-linked nanofiltration membrane synthesis, Thioether-based cross-linked free-standing film preparation, ^{1}H liquid

NMR study, FTIR analysis of the MPTMS precursor used in the vapor phase deposition grafting of the ceramic support, X-ray fluorescence spectroscopy (XRF), Cyclohexane permporometry analysis, Optimization of the VIP reaction parameters, FTIR analysis of free-standing film via liquid-liquid IP (LIP), PEG MWCO measurements for the Al-SiM/TE sample, Spectroscopic ellipsometry, Solvent filtration measurements and dye retention tests of the Al-SiM/TE membrane, TGA/DSC analysis (PDF)

AUTHOR INFORMATION

Corresponding Author

*Email: m.d.pizzoccaro@utwente.nl. Phone: +31 53 489 1506.

ORCID: Marie-Alix Pizzoccaro-Zilamy: 0000-0003-2496-099X

Funding Sources

This work is part of the research program titled “Solvent Tolerant Nanofiltration and Reverse Osmosis membranes for the purification of industrial aqueous streams” (BL-20-12), which is taking place within the framework of the Institute for Sustainable Process Technology (ISPT) and is partly financed by the Topsector Energy subsidy of the Ministry of economic affairs in The Netherlands. J.D.W acknowledges funding support from the ‘Vemieuwingsimpuls’ programme through project number VIDI 723.015.003 (financed by the Netherlands Organization for Scientific Research, NWO).

ACKNOWLEDGMENT

The authors declare no competing financial interest. The authors would like to thank Frank Morssinkhof of the Inorganic Membranes research group for providing technical assistance throughout this project and Mark Smithers of the Nanolab at the MESA+ Institute for the SEM imaging.

ABBREVIATIONS

NF, nanofiltration;

MWCO, molecular weight cut-off;

MPTMS, 3-mercaptopropyl)trimethoxysilane;

2SH, 1,3-benzenedithiol;

TEOA, triethanolamine;

BY, Brilliant Yellow;

RB, Rhodamine B;

SBB, Sudan Black B;

PEG, polyethylene glycol;

REFERENCES

(1) Marchetti, P.; Solomon, M. F. J.; Szekely, G.; Livingston, A. G. Molecular Separation with Organic Solvent Nanofiltration: A Critical Review. Chem. Rev. 2014, 114, 10735−10806. https://doi.org/10.1021/cr500006j.

(2) Vandezande, P.; Gevers, L. E. M.; Vankelecom, I. F. J. Solvent Resistant Nanofiltration: Separating on a Molecular Level. Chem. Soc. Rev. 2008, 37 (2), 365–405. https://doi.org/10.1039/b610848m.

(3) Szekely, G.; Jimenez-Solomon, M. F.; Marchetti, P.; Kim, J. F.; Livingston, A. G. Sustainability Assessment of Organic Solvent Nanofiltration: From Fabrication to Application. Green Chem. 2014, 16 (10), 4440–4473. https://doi.org/10.1039/c4gc00701h.

(4) Wittbecker, E. L.; Morgan, P. W. Interfacial Polycondensation. I. J. Polym. Sci. Part A Polym. Chem. 1996, 34 (4), 521–529. https://doi.org/10.1002/pola.1996.815.

(5) Gong, G.; Wang, P.; Zhou, Z.; Hu, Y. New Insights into the Role of an Interlayer for the Fabrication of Highly Selective and Permeable Thin-Film Composite Nanofiltration Membrane. ACS Appl. Mater. Interfaces 2019, 11 (7), 7349–7356. https://doi.org/10.1021/acsami.8b18719.

(6) Raaijmakers, M. J. T.; Benes, N. E. Current Trends in Interfacial Polymerization Chemistry. Prog. Polym. Sci. 2016, 63, 86–142. https://doi.org/10.1016/j.progpolymsci.2016.06.004.

(7) Song, Y.; Fan, J. B.; Wang, S. Recent Progress in Interfacial Polymerization. Mater. Chem. Front. 2017, 1 (6), 1028–1040. https://doi.org/10.1039/c6qm00325g.

(8) Mehta, P. P.; Pawar, V. S. Electrospun Nanofiber Scaffolds: Technology and Applications. In Applications of Nanocomposite Materials in Drug Delivery; Elsevier, 2018; pp 509–573. https://doi.org/10.1016/B978-0-12-813741-3.00023-6.

(9) Lee, K. P.; Bargeman, G.; de Rooij, R.; Kemperman, A. J. B.; Benes, N. E. Interfacial Polymerization of Cyanuric Chloride and Monomeric Amines: PH Resistant Thin Film Composite Polyamine Nanofiltration Membranes. J. Memb. Sci. 2017, 523, 487–496. https://doi.org/10.1016/J.MEMSCI.2016.10.012.

(10) Jye, L. W.; Ismail, A. F. Nanofiltration Membranes; CRC Press, 2016. https://doi.org/10.1201/9781315181479.

(11) Do, V. T.; Tang, C. Y.; Reinhard, M.; Leckie, J. O. Degradation of Polyamide Nanofiltration and Reverse Osmosis Membranes by Hypochlorite. Environ. Sci. Technol. 2012, 46 (2), 852–859. https://doi.org/10.1021/es203090y.

(12) Ma, Q.; Shuler, P. J.; Aften, C. W.; Tang, Y. Theoretical Studies of Hydrolysis and Stability of Polyacrylamide Polymers. Polym. Degrad. Stab. 2015, 121, 69–77. https://doi.org/10.1016/j.polymdegradstab.2015.08.012.

(13) Kolb, H. C.; Finn, M. G.; Sharpless, K. B. Click Chemistry: Diverse Chemical Function from a Few Good Reactions. Angew. Chemie Int. Ed. 2001, 40 (11), 2004–2021. https://doi.org/10.1002/1521-3773(20010601)40:11<2004::AID-ANIE2004>3.0.CO;2-5.

(14) Timmerman, P.; Beld, J.; Puijk, W. C.; Meloen, R. H. Rapid and Quantitative Cyclization of Multiple Peptide Loops onto Synthetic Scaffolds for Structural Mimicry of Protein Surfaces. ChemBioChem 2005, 6 (5), 821–824. https://doi.org/10.1002/cbic.200400374.

(15) Richelle, G. J. J.; Ori, S.; Hiemstra, H.; van Maarseveen, J. H.; Timmerman, P. General and Facile Route to Isomerically Pure Tricyclic Peptides Based on Templated Tandem CLIPS/CuAAC Cyclizations. Angew. Chemie Int. Ed. 2018, 57 (2), 501–505. https://doi.org/10.1002/anie.201709127.

(16) Monnereau, L.; Grandclaudon, C.; Muller, T.; Bräse, S. Sulfur-Based Hyper Cross-Linked Polymers. RSC Adv. 2015, 5 (30), 23152–23159. https://doi.org/10.1039/c5ra01463h.

(17) Rapakousiou, A.; Sakamoto, R.; Shiotsuki, R.; Matsuoka, R.; Nakajima, U.; Pal, T.; Shimada, R.; Hossain, A.; Masunaga, H.; Horike, S.; Kitagawa, Y.; Sasaki, S.; Kato, K.; Ozawa, T.; Astruc, D.; Nishihara, H. Liquid/Liquid Interfacial Synthesis of a Click Nanosheet. Chem. - A Eur. J. 2017, 23 (35), 8443–8449. https://doi.org/10.1002/chem.201700201.

(18) Salehi, H.; Shakeri, A.; Mahdavi, H.; Lammertink, R. G. H. Improved Performance of Thin-Film Composite Forward Osmosis Membrane with Click Modified Polysulfone Substrate. Desalination 2020, 496, 114731. https://doi.org/10.1016/j.desal.2020.114731.

(19) Cai, T.; Li, M.; Neoh, K. G.; Kang, E. T. Surface-Functionalizable Membranes of Polycaprolactone-Click-Hyperbranched Polyglycerol Copolymers from Combined Atom Transfer Radical Polymerization, Ring-Opening Polymerization and Click Chemistry. J. Mater. Chem. B 2013, 1 (9), 1304–1315. https://doi.org/10.1039/c2tb00273f.

(20) Xie, Y.; Tayouo, R.; Nunes, S. P. Low Fouling Polysulfone Ultrafiltration Membrane via Click Chemistry. J. Appl. Polym. Sci. 2015, 132 (21), n/a-n/a. https://doi.org/10.1002/app.41549.

(21) Liu, T.; Chen, D.; Cao, Y.; Yang, F.; Chen, J.; Kang, J.; Xu, R.; Xiang, M. Construction of a Composite Microporous Polyethylene Membrane with Enhanced Fouling Resistance for Water Treatment. J. Memb. Sci. 2021, 618, 118679. https://doi.org/10.1016/j.memsci.2020.118679.

(22) Arslan, M.; Pulido, B. A.; Nunes, S. P.; Yagci, Y. Functionalization of Poly(Oxindole Biphenylylene) Membranes by Photoinduced Thiol-Yne Click Chemistry. J. Memb. Sci. 2020, 598, 117673. https://doi.org/10.1016/j.memsci.2019.117673.

(23) Pujari, S. P.; Scheres, L.; Marcelis, A. T. M.; Zuilhof, H. Covalent Surface Modification of Oxide Surfaces. Angew. Chemie - Int. Ed. 2014, 53 (25), 6322–6356. https://doi.org/10.1002/anie.201306709.

(24) Zheng, Z.; Zhao, H.; Fa, W.; He, W.; Wong, K. W.; Kwok, R. W. M.; Lau, W. M. Construction of Cross-Linked Polymer Films Covalently Attached on Silicon Substrate via

a Self-Assembled Monolayer. RSC Adv. 2013, 3 (29), 11580–11585. https://doi.org/10.1039/c3ra40949j.

(25) Maaskant, E.; de Wit, P.; Benes, N. E. Direct Interfacial Polymerization onto Thin Ceramic Hollow Fibers. J. Memb. Sci. 2018, 550, 296–301. https://doi.org/10.1016/j.memsci.2018.01.009.

(26) R.J.R. Uhlhorn, M.H.B.J. Huis In't Veld, K. Keizer, A. J. B. Synthesis of Ceramic Membranes Synthesis of Non-Supported and Supported y-Alumina. J. Mater. Sci. 1992, 27, 527–537.

(27) ten Hove, M.; Luiten-Olieman, M. W. J.; Huiskes, C.; Nijmeijer, A.; Winnubst, L. Hydrothermal Stability of Silica, Hybrid Silica and Zr-Doped Hybrid Silica Membranes. Sep. Purif. Technol. 2017, 189, 48–53. https://doi.org/10.1016/j.seppur.2017.07.045.

(28) Abedini, S.; Parvin, N.; Ashtari, P.; Jazi, F. S. Microstructure, Strength and CO2 Separation Characteristics of α-Alumina Supported γ-Alumina Thin Film Membrane. Adv. Appl. Ceram. 2013, 112 (1), 17–22. https://doi.org/10.1179/1743676112Y.0000000043.

(29) Cuperus, F. P.; Bargeman, D.; Smolders, C. A. Permporometry: The Determination of the Size Distribution of Active Pores in UF Membranes. J. Memb. Sci. 1992, 71 (1–2), 57–67. https://doi.org/10.1016/0376-7388(92)85006-5.

(30) Yang, D.; Paul, B.; Xu, W.; Yuan, Y.; Liu, E.; Ke, X.; Wellard, R. M.; Guo, C.; Xu, Y.; Sun, Y.; Zhu, H. Alumina Nanofibers Grafted with Functional Groups: A New Design in Efficient Sorbents for Removal of Toxic Contaminants from Water. Water Res. 2010, 44 (3), 741–750. https://doi.org/10.1016/j.watres.2009.10.014.

(31) Coates, J. Interpretation of Infrared Spectra, A Practical Approach. In Encyclopedia of Analytical Chemistry; John Wiley & Sons, Ltd: Chichester, UK, 2006. https://doi.org/10.1002/9780470027318.a5606.

(32) Maaskant, E.; Gojzewski, H.; Hempenius, M. A.; Vancso, G. J.; Benes, N. E. Thin Cyclomatrix Polyphosphazene Films: Interfacial Polymerization of Hexachlorocyclotriphosphazene with Aromatic Biphenols. Polym. Chem. 2018, 9 (22), 3169–3180. https://doi.org/10.1039/c8py00444g.

(33) Khalili, F.; Henni, A.; East, A. L. L. PK a Values of Some Piperazines at (298, 303, 313, and 323) K. J. Chem. Eng. Data 2009, 54, 2914–2917. https://doi.org/10.1021/je900005c.

(34) Pepels, M.; Filot, I.; Klumperman, B.; Goossens, H. Self-Healing Systems Based on Disulfide-Thiol Exchange Reactions. Polym. Chem. 2013, 4 (18), 4955–4965. https://doi.org/10.1039/c3py00087g.

(35) Carrion-Vazquez, M.; Oberhauser, A. F.; Fowler, S. B.; Marszalek, P. E.; Broedel, S. E.; Clarke, J.; Fernandez, J. M. Mechanical and Chemical Unfolding of a Single Protein : Proc. Natl. Acad. Sci. 1999, 96 (March), 3694–3699.

(36) Saric, I.; Peter, R.; Kolympadi Markovic, M.; Jelovica Badovinac, I.; Rogero, C.; Ilyn, M.; Knez, M.; Ambrožić, G. Introducing the Concept of Pulsed Vapor Phase Copper-Free Surface Click-Chemistry Using the ALD Technique. Chem. Commun. 2019, 55 (21), 3109–3112. https://doi.org/10.1039/C9CC00367C.

(37) Gao, F.; Aminane, S.; Bai, S.; Teplyakov, A. V. Chemical Protection of Material Morphology: Robust and Gentle Gas-Phase Surface Functionalization of ZnO with Propiolic Acid. Chem. Mater. 2017, 29 (9), 4063–4071. https://doi.org/10.1021/acs.chemmater.7b00747.

(38) Lin-Vien, D.; Colthup, N. B.; Fateley, W. G.; Grasselli, J. G. The Handbook of Infrared and Raman Characteristic Frequencies of Organic Molecules; Daimay Lin-Vien, Colthup Norman B., Fateley William G., G. J. G., Ed.; Academic Press, 1991. https://doi.org/doi:10.1021/ac60293a718.

(39) Colthup, N. B.; Daly, L. H.; Wiberley, S. E. METHYL AND METHYLENE GROUPS. In Introduction to Infrared and Raman Spectroscopy; Elsevier, 1990; pp 215–233. https://doi.org/10.1016/b978-0-08-091740-5.50008-9.

(40) Benevides, P. J. C.; Young, M. C. M.; Giesbrecht, A. M.; Roque, N. F.; Da Bolzani, V. S. Antifungal Polysulphides from Petiveria Alliacea L. Phytochemistry 2001, 57 (5), 743–747. https://doi.org/10.1016/S0031-9422(01)00079-6.

(41) Benzyl sulfide https://webbook.nist.gov/cgi/cbook.cgi?ID=C538749&Type=IR-SPEC&Index=2#IR-SPEC (accessed Apr 8, 2020).

(42) Pizzoccaro-Zilamy, M. A.; Huiskes, C.; Keim, E. G.; Sluijter, S. N.; Van Veen, H.; Nijmeijer, A.; Winnubst, L.; Luiten-Olieman, M. W. J. New Generation of Mesoporous Silica Membranes Prepared by a Stöber-Solution Pore-Growth Approach. ACS Appl. Mater. Interfaces 2019, 11 (20), 18528–18539. https://doi.org/10.1021/acsami.9b03526.

(43) Puhlfürß, P.; Voigt, I.; Weber, R.; Morbé, M. Microporous TiO2membranes with a Cut off <500 Da. J. Memb. Sci. 2000, 174 (1), 123–133. https://doi.org/10.1016/S0376-7388(00)00380-X.

(44) Singh, S.; Khulbe, K. C.; Matsuura, T.; Ramamurthy, P. Membrane Characterization by Solute Transport and Atomic Force Microscopy. J. Memb. Sci. 1998, 142 (1), 111–127. https://doi.org/10.1016/S0376-7388(97)00329-3.

(45) Pinheiro, A. F. M.; Hoogendoorn, D.; Nijmeijer, A.; Winnubst, L. Development of a PDMS-Grafted Alumina Membrane and Its Evaluation as Solvent Resistant Nanofiltration Membrane. J. Memb. Sci. 2014, 463, 24–32. https://doi.org/10.1016/J.MEMSCI.2014.03.050.

(46) Maaskant, E.; Vogel, W.; Dingemans, T. J.; Benes, N. E. The Use of a Star-Shaped Trifunctional Acyl Chloride for the Preparation of Polyamide Thin Film Composite Membranes. J. Memb. Sci. 2018, 567, 321–328. https://doi.org/10.1016/j.memsci.2018.09.032.

(47) Gothe, P. K.; Gaur, D.; Achanta, V. G. MPTMS Self-Assembled Monolayer Deposition for Ultra-Thin Gold Films for Plasmonics Related Content. J. Phys. Commun. 2018, 2 (3), 035005. https://doi.org/10.1088/2399-6528/aaaedd.

SYNOPSIS